The role of water in N_2O anion dissociation and reaction rates of N_2O with hydrated electrons in high temperature water

Kenji Takahashi[1*], David M. Bartels[2] and Charles D. Jonah [3]

[1]Department of Chemistry and Chemical Engineering, Kanazawa University, Kanazawa 920-8667, Japan
[2] Notre Dame Radiation Laboratory, Notre Dame University, Notre Dame, Indiana 46556, USA
[3] Chemistry Division, Argonne National Laboratory, Argonne, IL60439, USA
[*]E-mail: ktkenji@t.kanazawa-u.ac.jp

Nitrous oxide (N_2O) is known as an important "greenhouse gas" but also a scavenger of hydrated electron and a source of OH radical. While there has been considerable interesting research on the electron attachment to N_2O in the gas phase, the presence of solvent molecules will significantly alter the electron affinity, molecular structure and chemical reactivity of N_2O. *Ab initio* calculations of the N_2O^- anion suggest that electron affinity of N_2O in gas phase is negative, while a positive value of electron affinity is recommended in a handbook. The calculations also suggest a possible dissociation path of N_2O^- anion in a gas phase and water. The reaction rate of hydrated electrons, $(e^-)_{aq}$, with N_2O can be fitted with an Arrhenius-type temperature dependence up to 300 °C with an activation energy of 15.5 kJ/mol. At higher temperatures, the rate constant decreases to give a local minimum at 380 °C.

1. Introduction

The reaction of nitrous oxide (N_2O) with hydrated electrons $(e^-)_{aq}$ has been widely used to convert $(e^-)_{aq}$ to OH radicals in water. The reduction of N_2O produces the N_2O^- anion, which dissociates to give O^- and N_2. The O^- anion immediately reacts with a water molecule to give OH radicals and OH^-[1].

$$(e^-)_{aq} + N_2O \rightarrow N_2O^- \quad (1)$$
$$N_2O^- \rightarrow N_2 + O^- \quad (2)$$
$$O^- + H_2O \rightarrow OH + OH^- \quad (3)$$

While there has been considerable interesting research on the electron attachment to N_2O in the gas phase [2-12], the presence of solvent molecules will significantly alter the electron affinity, molecular structure and chemical reactivity of N_2O. One cannot apply the gas phase data to an N_2O solution. A thermal electron is very unreactive with an isolated N_2O molecule in the gas phase[13], while in the condensed phase, this reaction is close to diffusion controlled. Thus, the effects that accelerate the gas phase-reaction are probably not relevant for the condensed-phase reaction. The differences between gas and condensed phase are not confined to N_2O solutions. For example, we have demonstrated for CO_2 molecules that the CO_2^- anion is unstable in the gas phase while the CO_2^- anion is stable in water and CO_2 dimer anion is stable in supercritical CO_2[14,15]. The reactivity of CO_2 and the CO_2^- anion in a high-density supercritical CO_2 is significantly different from that in gas phase.

In this study, we report the reaction rate of $(e^-)_{aq}$ with N_2O in high temperature water, including the supercritical regime. We also report *ab initio* calculations used to explore the potential energy curves of the N_2O^- anion in water. A possible dissociation path of the N_2O^- anion and its energetics in water will be discussed.

2. Experimental

2.1. Pulse radiolysis The experimental system is basically the same as previously described [16] except for the electron accelerator used. We shall only give an outline of the experimental system; please see the cited references for further details.
Electron pulse radiolysis experiments were carried out using the 45 MeV Linac installed at Hokkaido University. Kinetics were measured by injecting a 10-ns electron pulse and monitoring the optical absorption of $(e^-)_{aq}$ at 800 nm. A pulsed 300-W xenon-arc lamp provided the probe light, and the wavelength was isolated using a 10-nm bandwidth

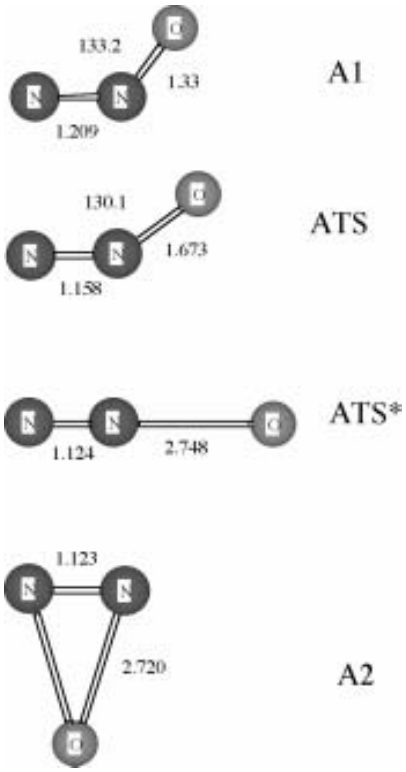

Fig. 1. Optimized geometries of the N_2O^- anion in the gas phase. Bond lengths and angles shown are values reported by Kryachko *et al*.

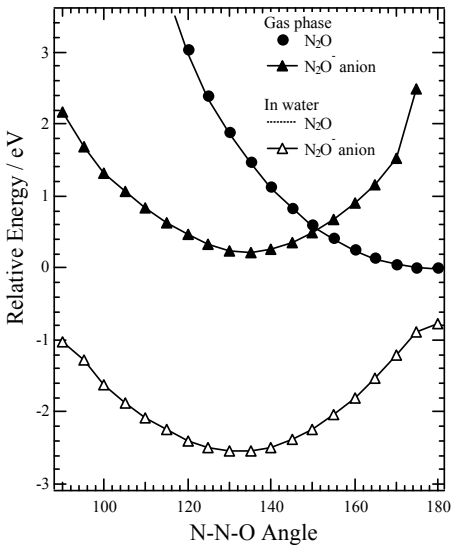

Fig. 2. Potential energy surfaces of N_2O and the N_2O^- anion in the gas phase and water as a function of N-N-O angle. The potential surface for N_2O in water (dashed line) is nearly indistinguishable from the potential surface of N_2O in gas phase (filled circle).

interference filter. The probe light was detected with a reverse-biased photodiode (EG&G FND100), and data were acquired using a digital oscilloscope (LeCroy model 9362). Data analysis was carried out using standard non-linear least-square-fitting techniques.

The high-pressure cell used for these measurements has been previously described [16]. Stock solutions of water purged with N_2O at 1 atm were mixed with degassed pure water using two separate HPLC pumps (JASCO PU-980). The flow rates of the pumps at high pressure were calibrated by weighing the amount of water pumped over the course of one minute. The total flow rate was kept constant (normally 4 ml/min) to maintain a stable temperature and pressure in the sample cell. Five to twenty decay signals of the hydrated electrons were averaged, depending on the temperature. The pseudo-first-order reaction rates were measured using four or five different N_2O concentrations (ranging from 10 to 400 □M). The molal scavenger concentration was calculated from the relative flow rates of the HPLC pumps. The final molar concentration was calculated from the density of water at the experimental temperature and pressure.

2.2. *Ab initio* calculations *Ab initio* calculations of the N_2O^- anion were performed using GAUSSIAN 98 [17]. The geometries were initially optimized using B3LYP/(aug)-cc-pVDZ methods. The energies were further refined using quadratic configuration interaction, QCISD(T), in conjunction with the (aug)-cc-pVDZ basis set. Solvation effects were simulated using the polarized continuum model (PCM) of Tomasi and coworkers [18], which is available as a self-consistent reaction field (SCRF) theory in GAUSSIAN 98.

3. Results and Discussion

3.1. Potential energy curve of N_2O^- anion in water There are several questions regarding the nature of the N_2O^- anion. These include: 1) the threshold for dissociative electron attachment and 2) the electron affinity. Even though established thermodynamic measurements calculate a value for the threshold for dissociative electron of 0.26 eV,

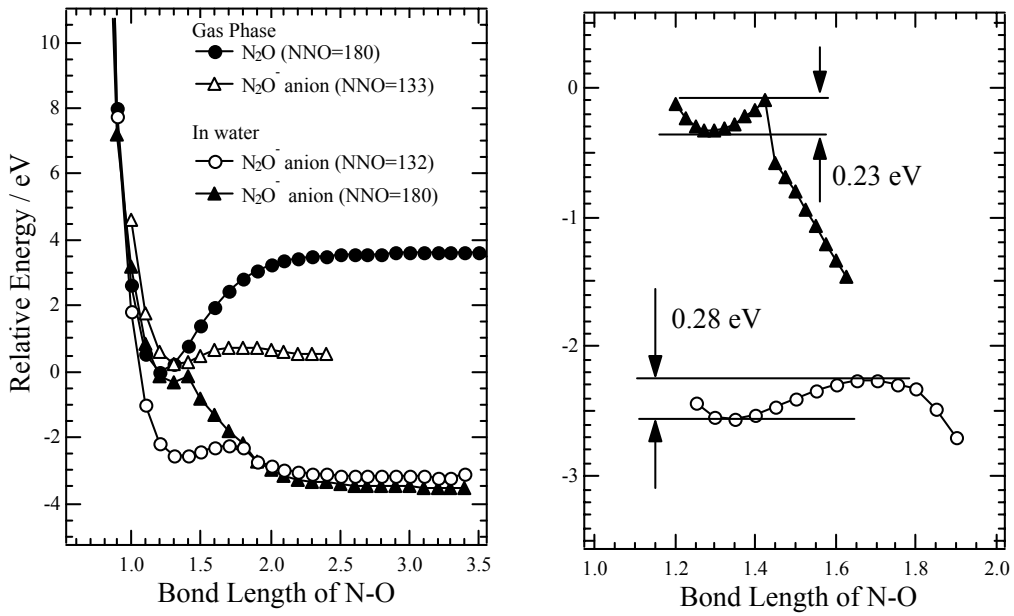

Fig. 3. Potential energy curves of N_2O and N_2O^- anion in the gas phase and water as a function of N-O bond length.

most gas phase experiments observe an O^- signal at 0 eV[6]. This disparity was resolved by Chantry, who showed that the results depend on pressure [26]. While the adiabatic electron affinity of N_2O in the gas phase is assigned to be +0.22 eV [8], there are both experimental and theorical results on the electron affinity that disagree with this value [for example, 9-11], and the reason for this disparity has not been determined.

For N_2O^- formed in water, our understanding is very limited. There is no information on the electron affinity, structure of the anion, and the potential curves for dissociation of the anion. For this reason we firstly examined the solvent effect on stability and dissociation of the N_2O^- anion.

It is known that the N_2O^- anion has a bent form with an N-N-O bond angle of about 133° in the gas phase [12]. The bond lengths of N-O and N-N are stretched as compared with the neutral species. Recently, Kryachko *et al.* performed extensive *ab initio* calculations on N_2O and N_2O^- using a aug-cc-pVQZ basis set at the coupled-cluster level, CCSD(T) [12]. According to their calculations, the N_2O^- anion lies 0.26 eV *above* neutral N_2O in gas phase. They found two transition states of the N_2O^- anion as shown in fig. 1 (ATS and ATS*).

We have confirmed the negative (adiabatic) electron affinity of N_2O in gas phase at the QCISD(T)/aug-cc-pVDZ level. Fig. 2 shows the potential energy of the N_2O^- anion in the gas phase and in PCM "water" as a function of the N-N-O bond angle. The zero of energy was defined as the ground state of N_2O in the gas phase. The N-N and N-O bond lengths were fixed as 1.185 and 1.302 Å, respectively. In the gas phase, the energy of the N_2O^- anion in its relaxed (bent) form is 0.16 eV *above* the ground state of linear neutral N_2O. The lowest point of crossing between the energy curves of the N_2O^- anion and N_2O occurs at a bond angle of about 150°. The potential barrier for the electron autodetachment is 0.45 eV. Conversely, in water the energy of the bent N_2O^- anion is 2.5 eV *below* the ground state of neutral N_2O with bond lengths N-N = 1.196 Å and N-O = 1.311 Å. Even in a non-relaxed linear form of the N_2O^- anion, the energy is 0.7 eV *below* the ground state of N_2O. Hence in water the electron attachment to N_2O is energetically favorable.

In both the gas phase and in water, it is known that the N_2O^- anion dissociates into N_2 and O^- after electron attachment [1]. Consequently, we now turn to the potential energy of the N_2O^- anion as a

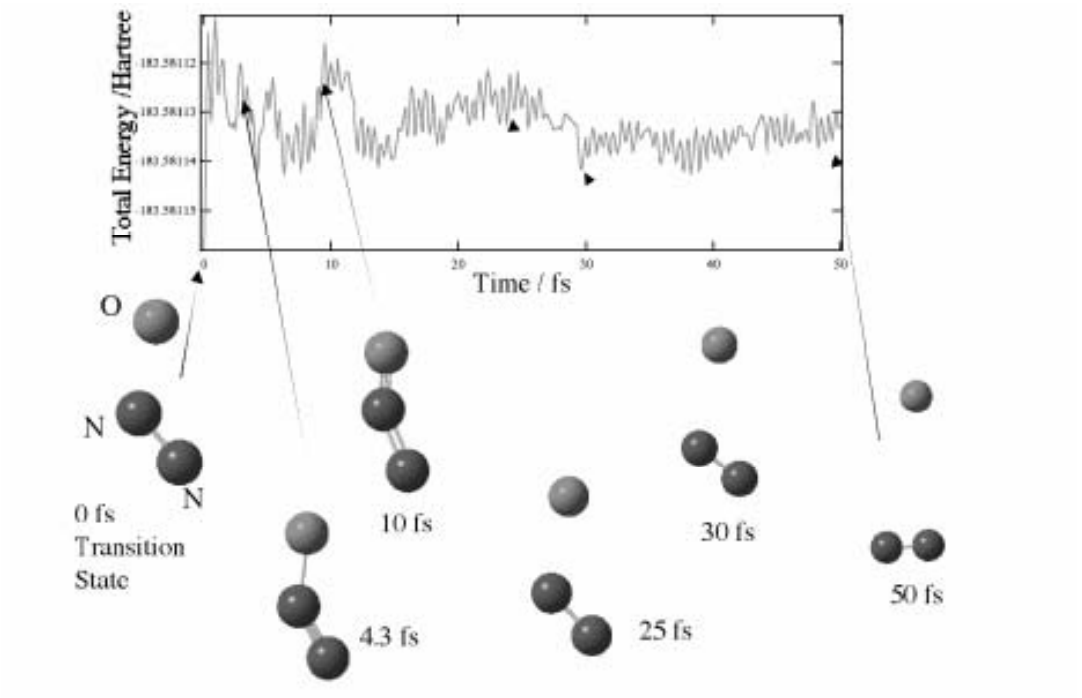

Fig. 4. *Ab initio* molecular dynamics of N_2O^- anion dissociation in gas phase.

function of the N-O bond length. We calculated the potential energy curves for two selected N-N-O bond angles of 180° and 132°. The results are shown in fig. 3. Let us first consider the potential energy curve of the N_2O^- anion in water. For the potential energy with N-N-O = 180°, a minimum (-0.33 eV) is located at a N-O bond length of 1.3 Å. With increasing bond length, the energy increases, and then sharply drops at a bond length of 1.45 Å. The energy difference between the local minimum and the sharp "peak" is 0.23 eV. If the vibrational excitation energy exceeds this potential barrier, the N_2O anion will easily dissociate into N_2 and O^-.

For the potential energy curve with a N-N-O angle of 132°, a broad potential barrier for dissociation into N_2 and O^- was found at a bond length of about 1.7 Å, and a local minimum was found at a bond length of about 1.3 Å. The energy difference between the local minimum and the broad potential barrier is 0.28 eV. Both of the bond angles selected for calculations indicate that only a small energy (0.21 to 0.28 eV) is required to overcome the potential barrier for the dissociation of the N_2O^- anion in water.

Kryachko *et al.* [12] reported two different geometries for the N_2O^- anion in the gas phase. One is a well-known bent form (A1 in fig.1), and another is a cyclic structure with long N-O bond lengths (A2 in fig.1). They suggested that following electron attachment, the N_2O system undergoes a facile dissociation process through the cyclic isomer to the final fragments, $e^- + N_2O \rightarrow$A1 (0.26 eV)$\rightarrow$□□S(0.52 eV) $\rightarrow$ A2(0.03 eV) $\rightarrow N_2 + O^-$. The numbers in parentheses are energies relative to the ground state of neutral N_2O.

In case of the N_2O^- anion in water, an optimized cyclic geometry was obtained. However, the bond length of N-O is 3.5 Å, suggesting that the O^- is almost dissociated from the N_2O system at this geometry. Therefore, we think that following the electron attachment in water, the N_2O^- anion will change geometry to the bent form and then dissociate through the small potential barrier shown in fig. 3.

In fig. 4, *ab initio* calculations for molecular dynamics of N_2O^- anion dissociation in gas phase are shown. The calculations were performed with DFT/B3LYP level, and started from the transition

state of N_2O^- anion. Within 10 fs the N-O bond is shortened because of the vibration of the bond. However after 10 fs the N-O bond stretched and O^- dissociate from N_2. At 50 fs O^- completely dissociate from N_2.

3.1. Reaction rate of hydrated electrons with N_2O in water In recent pulse radiolysis/optical absorption work, the reaction of N_2O with $(e^-)_{aq}$ was used to study reactions of OH radicals with several solutes under both sub- and supercritical water conditions [20-23]. It is widely acknowledged that OH radical reactions play an important role in supercritical water oxidation [24]. To make intelligent use of N_2O as an $(e^-)_{aq}$ scavenger and a source of OH radicals, knowledge of the reaction rate constant of $(e^-)_{aq}$ with N_2O is necessary over a wide range of temperatures, exceeding the critical temperature of water.

Examples of the $(e^-)_{aq}$ decay signals in 300 °C water are shown in Fig. 5. Solid lines are pseudo-first-order fits to the observed decay signals. The pseudo-first-order reaction rates were measured using four or five different N_2O concentrations (ranging from 10 to 400 □M). Fig. 6 shows an Arrhenius plot for the reaction of $(e^-)_{aq}$ with N_2O at a constant pressure of 260 bar. The rate constant essentially shows Arrhenius behavior up to 300°C. Above 300°C, the rate constant gradually decreases and gives a very sharp "dip" at 380 °C, after which it increases again. This behavior can be explained by considering the nature of solvent clustering and local density enhancements in supercritical water. Near the critical region, the entropic driving force that favors vaporization roughly balances the attractive potential between the solvent molecules responsible for condensation. Microclusters of molecules are constantly forming and dissipating. In this environment, solute molecules with attractive potential relative to the solvent will tend to form the nucleus of a cluster and be found in a region of local density enhancement relative to the bulk average. A solute with repulsive potential can be expected to be found more often in the voids between the dynamic solvent clusters [25]. In our previous work [26], we interpreted our results by assuming that the hydrated electron in 380 °C water will strongly solvate within water clusters while hydrophobic molecules will be segregated in the voids between dynamic water clusters. On average, a potential of mean force develops to prevent reactive contact between the hydrated electron and hydrophobic species.

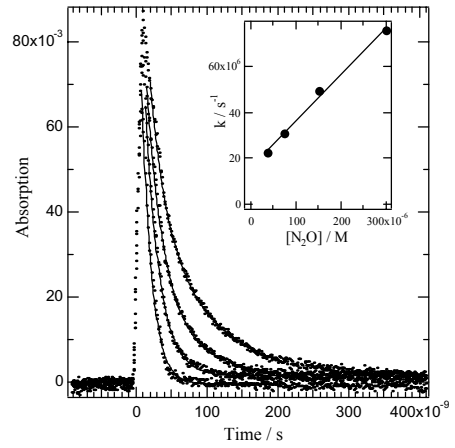

Fig. 5. Sample decay signals for hydrated electron scavenging by N_2O in 300 °C and 260 bar of water. Solid lines are fitting results. Inset: pseudo-first-order plot illustrating the concentration dependence of the observed scavenging rate at 300 °C.

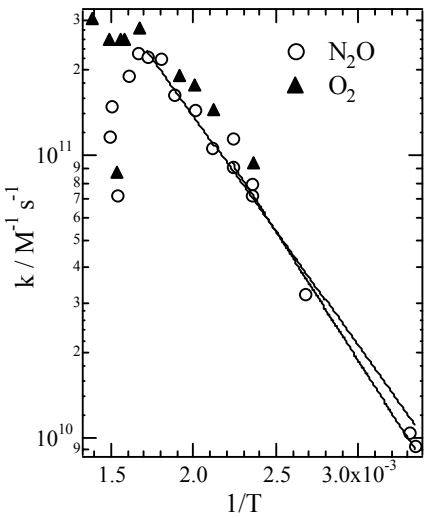

Fig. 6. Arrhenius plot for the reaction of the hydrated electron with N_2O. A solid line indicates a fit up to 300 °C, and the dashed line is a fit up to 150 °C. Reaction rates of the hydrated electron with O_2 (ref 26) are also plotted for comparison.

Fitting the rate constants over the temeprature range from 30 °C to 300 °C gives an activation energy of 15.5 ± 1.5 kJ/mol. The slight curvature in the Arrhenius plot will give a higher activation

energy if we fit the lower temperature data. A fit of the rate constants between room temperature and 150 °C gives an activation energy of 18.6 ± 1.5 kJ/mol (0.19 eV).

A similar activation energy for the reaction of $(e^-)_{aq}$ with oxygen (14.0 kJ/mol) was previously obtained [26]. In Fig. 6, the rate constant for the reaction of $(e^-)_{aq}$ with oxygen (at 250 bar) is also plotted for comparison. Up to 300 °C, the reaction rate constant of $(e^-)_{aq}$ with N_2O is slightly smaller than that for oxygen. The activation energy for the diffusion of $(e^-)_{aq}$ in water measured up to 100 °C is 20.3 kJ/mol [27], and previous studies of the reaction of $(e^-)_{aq}$ with nitrobenzene indicate an activation energy of 20.8 kJ/mol up to 300 °C [28]. Hence, the reaction of $(e^-)_{aq}$ with N_2O at higher temperatures is not diffusion-limited.

4. Conclusions

The reaction of N_2O with $(e^-)_{aq}$ in supercritical water shows similar behavior to that seen previously for the reaction of gases in high-temperature and supercritical water. *Ab initio* calculations of the N2O- anion suggest that electron affinity of N2O in gas phase is negative, while the anion is energeticaly stable in water.

Acknowledgements

Acknowledgment is made to Argonne National Laboratory, The Department of Energy and the Ministry of Education in Japan for financial support to K.T.

References and Notes

[1] E. J. Hart and M. Anbar, *The Hydrated Electron*, (Wiley Interscience, New York, 1970).
[2] G. J. Schulz, *J. Chem. Phys*., 34(1961) 1778
[3] D. Rapp, D. D. Briglia, *J. Chem. Phys*., **43**, 1480 (1965)
[4] A. D. Bass, M. Lezius, P. Ayotte, L. Parenteau, P. Cloutier, L. Sanche, *J. Phys. B*: *At. Mol. Opt. Phys*., **30**, 3527 (1997)
[5] M. N. Hedhill, R. Azria, Y. Le Coat, M. Tronc, *Chem. Phys. Lett*., **268**, 21 (1997)
[6] F. Brüning, S. Matejcik, E. Illenberger, Y. Chu, G. Senn, D. Muigg, G. Denifl, T. D. Märk, *Chem. Phys. Lett*., **292**, 177 (1998)
[7] E. Leber, S. Barsotti, J. Bommels, J. M. Weber, I. I. Fabrikant, M. –W. Ruf, H. Hotop, *Chem. Phys. Lett*., **325**, 345 (2000)
[8] D. G. Hopper, A. C. Wahl, R. L. C. Wu, T. O. Tiernan, *J. Chem. Phys*., **65**, 5474 (1976)
[9] D. R. Yarkpny, *J. Chem. Phys*., **78**, 6763 (1983)
[10] D. Yu, A. Rauk, D. A. Armstrong, *J. Phys. Chem*., **96**, 6013 (1992)
[11] M. C. McCarthy, J. W. R. Allington, K. O. Sullivan, *Mol. .Phys*., **96**, 1735 (1999)
[12] E. S. Kryachko, C. Vinckier, and M. T. Nguyen, *J. Chem. Phys*., **114**, 7911 (2001)
[13] R. S. Dixon and M. G. Bailey, *Can. J. Chem* **46**, 1181 (1968)
[14] K. Takahashi, S. Sawamura, N. M. Dimitrijevic, D. M. Bartels, C. D. Jonah, *J. Phys. Chem. A*, **106**, 108 (2002)
[15] I. A. Shkrob, M. C. Sauer, Jr., C. D. Jonah, K. Takahashi, *J. Phys. Chem. A* , **106**, 11855 (2002)
[16] K. Takahashi, J. A. Cline, D. M. Bartels and C. D. Jonah, Rev. Sci. Inst., **71**, 3345 (2000)
[17] Gaussian 98, Revision A.11.1, M. J. Frisch et al., Gaussian, Inc., Pittsburgh PA, 2001.
[18] For example; J. Tomashi, *Chem. Rev*., **94**, 2027 (1994)
[19] P. J. Chantry, *J. Chem. Phys*., **51**, 3369 (1969)
[20] J. L. Ferry and M. A. Fox, *J. Phys. Chem. A*, **102**, 3705 (1998)
[21] J. L. Ferry and M. A. Fox, *J. Phys. Chem. A*, **103**, 3438 (1999)
[22] G. Wu, Y. Katsumura, Y. Muroya, M. Lin, and T. Morioka, *J. Phys. Chem. A*, **105**, 4933 (2001)
[23] G. Wu, Y. Katsumura, Y. Muroya, M. Lin, and T. Morioka, *J. Phys. Chem. A*, **106**, 2430 (2002)
[24] For example, P. E. Savage, *Chem. Rev*., **99**, 603 (1999)
[25] I. B. Petsche, P. G. Debenedetti, *J. Phys. Chem*., **95**, 386 (1991)
[26] J. A. Cline, K. Takahashi, T. W. Marin, C. D. Jonah and D. M. Bartels, *J. Phys. Chem. A*, **106**, 12260 (2002)
[27] K. H. Schmidt, P. Han, and D. M. Bartels, *J. Phys. Chem*., **99**, 10530 (1995)
[28] T. W. Marin, J. A. Cline, K. Takahashi, D. M. Bartels, and C. D. Jonah, *J. Phys. Chem. A*, **106**, 12270 (2002)